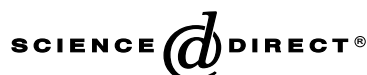


Available online at www.sciencedirect.com**DEVELOPMENTAL
BIOLOGY**

Developmental Biology 261 (2003) 470–487

www.elsevier.com/locate/ydbio

Dynamic morphogenetic events characterize the mouse visceral endoderm

Jaime A. Rivera-Pérez, Jesse Mager, and Terry Magnuson*

Department of Genetics, University of North Carolina, 103 Mason Farm Road, Chapel Hill, NC 27599-7264, USA

Received for publication 7 August 2002, revised 9 May 2003, accepted 9 May 2003

Abstract

Several lines of evidence suggest that the extraembryonic endoderm of vertebrate embryos plays an important role in the development of rostral neural structures. In mice, neural inductive signals are thought to reside in an area of visceral endoderm that expresses the *Hex* gene. Here, we have conducted a morphological and lineage analysis of visceral endoderm cells spanning pre- and postprimitive streak stages. Our results show that *Hex*-expressing cells have a tall, columnar epithelial morphology, which distinguishes them from other visceral endoderm cells. This region of visceral endoderm thickening (VET) is found overlying first the distal and then one side of the epiblast at stages between 5.5 and 5.75 days post coitum (d.p.c.). In addition, we show that the epiblast has an anteroposterior-compressed appearance that is aligned with the position of the VET. Intracellular labeling of VET/*Hex*-expressing cells reveals an anterior and anterolateral shift from their distal epiblast position. VET/*Hex*-expressing cells are first localized to the anterior side of the epiblast by 5.75 d.p.c. and form a crescent on the anterior half of the embryo at the onset of gastrulation. Subsequently, VET descendants are distributed along the embryonic/extraembryonic boundary by headfold stages at 7.5 d.p.c. The morphological characteristics and position of VET/*Hex*-expressing cells distinguishes the future anteroposterior axis of the embryo and provide landmarks to stage mouse embryos at preprimitive streak stages. Moreover, the morphological characteristics of pregastrulation mouse embryos together with the stereotyped shift in the position of visceral endoderm cells reveal similarities among amniote embryos that suggest an evolutionary conservation of the mechanisms that pattern the rostral neur ectoderm at pregastrula stages.

© 2003 Elsevier Inc. All rights reserved.

Keywords: Mouse; Gastrulation; Visceral endoderm; *Hex*; Iontophoresis; AVE

Introduction

The generation of the body plan in vertebrates requires morphogenetic and inductive events that define the axes of symmetry at early stages of embryogenesis (see reviews by Eyal-Giladi, 1997; Lu et al., 2001; Zernicka-Goetz, 2002). Once the primary axes have been established, further developmental processes lead to the regionalization of the embryo. One of the main events occurring in early embryogenesis is the induction and patterning of the neural plate. In several vertebrates, evidence suggests that the extraembryonic endodermal component of the pregastrula embryo plays an important role in the specification of the anterior

neur ectoderm. In anamniote embryos, the initial steps of neurogenesis are thought to rely on mesodermal derivatives generated during gastrulation, however, evidence from zebrafish and *Xenopus* embryos suggest that other tissues provide signals that impart anterior identity to the overlying ectoderm before the formation of the organizer (Ho et al., 1999; Jones et al., 1999; see reviews by Harland, 2000; Wilson and Edlund, 2001). In amniotes, the anterior visceral endoderm (AVE) of mouse embryos is believed to provide signals necessary for the correct definition of the rostral neur ectoderm (Thomas and Beddington, 1996). Similar signaling events have been proposed for the endoderm of the anterior marginal crescent of preprimitive streak rabbit embryos (Knoetgen et al., 1999). In chick embryos, the hypoblast has been suggested to provide signals and direct cell movements that pattern the forebrain (Foley et al., 2000, and

* Corresponding author. Fax: +1-919-843-6365.

E-mail address: trm4@med.unc.edu (T. Magnuson).

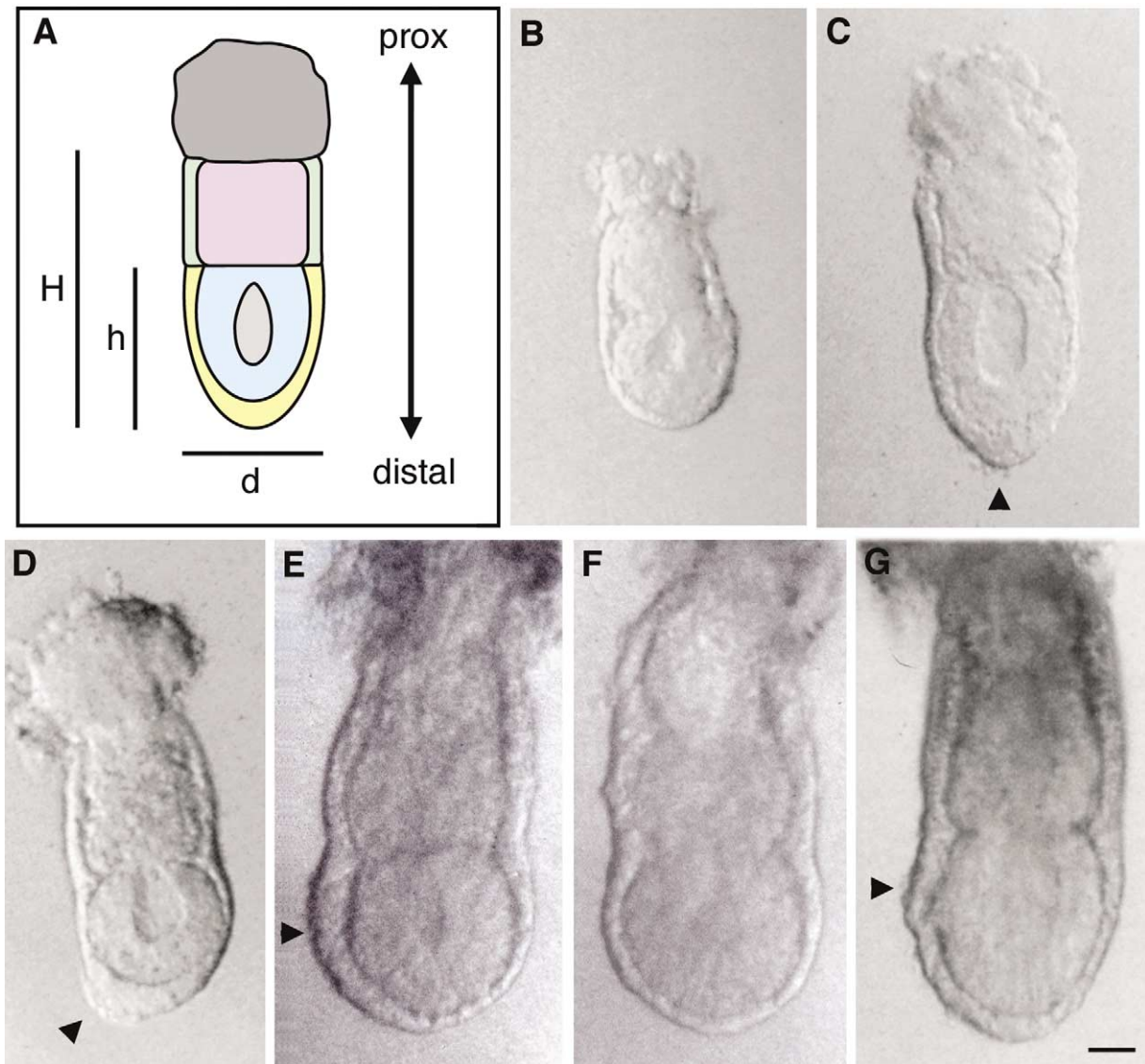


Fig. 1. Morphological asymmetry in visceral endoderm cells of embryos dissected between E5.5 and E5.75 d.p.c. (A) Schematic representation of a pregastrula embryo indicating its different components (the parietal yolk sac is not shown). Blue, epiblast; yellow, visceral endoderm adjacent to epiblast; purple, extraembryonic ectoderm; green, visceral endoderm adjacent to extraembryonic ectoderm; light gray, proamniotic cavity and dark gray, ectoplacental cone. H, denotes egg cylinder length; h, embryonic length; d, embryonic diameter. (B) One of the smallest embryos dissected illustrating a homogeneous morphology of the visceral endoderm. (C) Embryo showing a cap of tall columnar visceral endoderm epithelium at the distal tip of the egg cylinder (arrowhead). The cells are at least twice as tall as the cells covering the side of the epiblast. The proamniotic cavity has not expanded into the extraembryonic ectoderm. (D) Embryo showing an area of visceral endoderm thickening located to one side of the distal tip of the egg cylinder (arrowhead). The proamniotic cavity extends into the extraembryonic ectoderm. (E, F) Embryo showing a thickening of the visceral endoderm epithelium on one side of the epiblast (arrowhead in E). (E) The embryo in a side view; (F) After rotation of the egg cylinder 90° around its proximodistal axis. The area of tall columnar cells extends from the epiblast/extraembryonic ectoderm boundary to the tip of the egg cylinder and covers a maximum of half of the surface of the epiblast. (G) One of the largest embryos dissected. The VET is less conspicuous and abuts the epiblast/extraembryonic ectoderm boundary of the egg cylinder (arrowhead). All embryos are shown at the same magnification. Scale bar, 30 μ m. The double arrow in (A) indicates the proximodistal axis of the embryo.

references herein). These and other studies have led to the proposal that both the extraembryonic endoderm and mesodermal derivatives of the node have a synergistic role in the generation of anterior neural tissues (Beddington and Robertson, 1998; Shawlot et al., 1999; Tam and Steiner, 1999; Foley et al., 2000).

Among mammals, mice are the preferred species for

genetic and embryological studies; however, the focus of embryological research has been on embryos at preimplantation stages (see Gardner, 1997; Piotrowska and Zernicka-Goetz, 2001) or at postimplantation stages at the onset of gastrulation (see Beddington, 1994; Tam and Steiner, 1999). Nonetheless, the proposed role of the AVE in anterior neural patterning and the discovery that several molec-

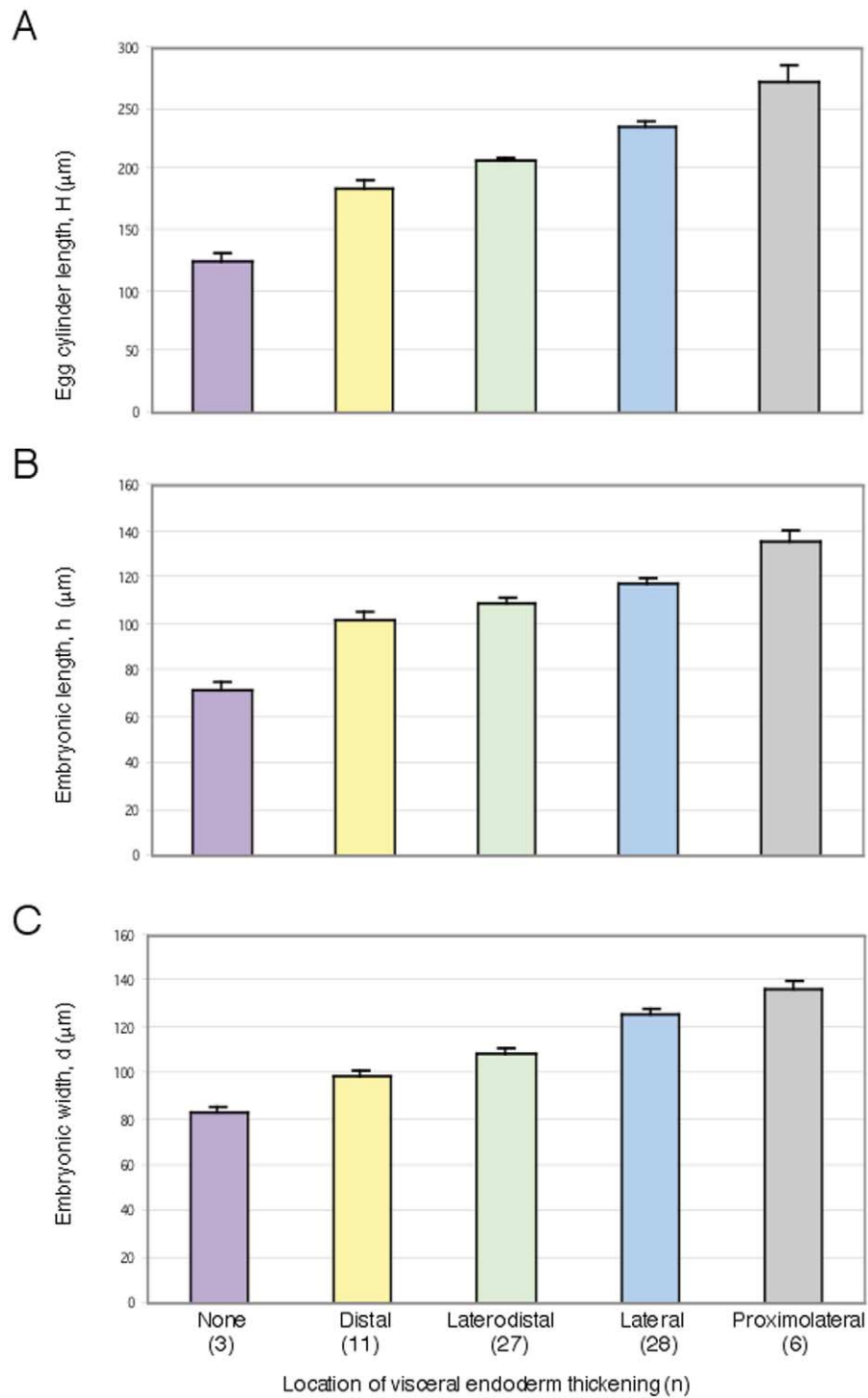


Fig. 2. Comparison of embryonic dimensions in embryos grouped according to the position of the visceral endoderm thickening. The average size of the egg cylinder length (H), embryonic length (h), and embryonic width (d) increased in accordance with the position of the VET. The standard error is shown as bars on top of each column. A simple regression analysis revealed a linear relationship amongst the dimensions of the different portions of the egg cylinder. $h = 0.516H$ (s.e. 0.0047, 95% CI: 0.517, 0.522); $d = 0.522H$ (s.e. 0.052, 95% CI: 0.517, 0.537); and $d = 0.967h$ (s.e. 0.0112, 95% CI: 0.945, 0.989).

ular markers are expressed asymmetrically in the preprimitive streak embryo (Rosenquist and Martin, 1995; reviewed by Beddington and Robertson, 1998) have refocused attention on the visceral endoderm of pregastrulation embryos,

from the time of implantation to the appearance of the primitive streak.

To gain insight into the morphogenetic role played by the visceral endoderm in the generation of anterior neural struc-

tures, we conducted a morphological and lineage analysis of visceral endoderm cells at pre- and postprimitivestreak stages. Our results show that a group of *Hex*-expressing cells, which are thought to provide signals for the development of the rostral neur ectoderm, has a distinctive morphology and undergoes dynamic positional shifts from the distal tip of the epiblast to the embryonic/extraembryonic boundary. These results provide essential tools to study the mechanisms that shape the mouse embryos at early postimplantation stages and reveal similarities among the extraembryonic tissues of developing amniote embryos, suggesting that evolutionary conserved mechanisms pattern the rostral neural structures of vertebrates.

Materials and methods

Mouse strains and dissection

Wild-type embryos were collected from CD-1 mice obtained from Charles River Laboratories. Heterozygous *Tg(Hex-eGFP)ARbe* embryos (Rodríguez et al., 2001) were obtained from crosses between mixed stock heterozygous males and CD-1 females. Dissection was performed in MEM α (Gibco) containing 20 mM Hepes, 10% FCS, and penicillin (100 U/ml)/Streptomycin (100 μ g/ml) using forceps. Dissected embryos were examined on a Nikon diaphot microscope equipped with DIC optics and epifluorescence at 300 \times magnification. Embryos with any obvious mechanical damage or an extremely bent ectoplacental cone were not considered for further study. Embryos were photographed by using a CCD camera (DAGE-MTI Inc. RC300). Embryonic dimensions were determined by measuring photographs using a millimeter scale and extrapolating to micrometers. Measurements of several images of the same embryo were averaged. The statistical analysis was done by using SAS system version 8.2.

Immunofluorescence and confocal analysis

Heterozygous *Tg(Hex-eGFP)ARbe* embryos dissected between 5.5 and 5.75 d.p.c. were fixed in 4% paraformaldehyde for 3 h or overnight at 4°C. After fixation, they were washed three times in PBS for 5 min incubated in blocking solution (5% goat serum, 1% BSA, 0.5% Triton X-100 in PBS) for 1 h, and then incubated overnight in primary antibody solution [rat anti-E-cadherin IgG (Zymed Cat No. 13-1900) diluted 1:500 in blocking solution] overnight at 4°C. After primary antibody staining, embryos were washed three times in blocking solution and incubated in secondary antibody solution [Alexa Fluor 594 goat anti-rat IgG (Molecular Probes Cat. No. A-11007) diluted 1:500 in PBT (1% BSA, 0.5% Triton X-100 in PBS)] for 1 h. Embryos were then rinsed three times in PBT and once in PBS for 5 min

and counterstained with a 2- μ g/ml aqueous solution of DAPI (4', 6-diamidino-2-phenylindole, dihydrochloride) for 2 min. Stained embryos were imaged by using a laser scanning confocal microscope (Leica SP2 AOBS) using a 63 \times /1.2 NA Apo water immersion objective. Optical sections were obtained every 2 μ m.

Embryo culture and iontophoretic injections

Labeled embryos with distal VET were cultured in hanging drops of 100% rat serum as follows: A drop of 90 μ l of rat serum was placed in the inner cavity of the cap of a 5-ml snap-cap polystyrene tube (Falcon Cat. No. 352058). One labeled embryo was added to the drop of serum and the cap was repositioned loosely on top of the tube containing 4 ml of PBS to avoid desiccation. All labeled embryos with lateral VET were cultured in media containing 80% rat serum and MEM α (Gibco). Lateral VET embryos cultured to preprimitivestreak stages were cultured in hanging drops as mentioned above. Lateral VET embryos cultured to primitivestreak stages were cultured either in four-well plates (Hyclone) containing 750 μ l of media or in rotating snap-cap tubes containing 500 μ l of media in a standard tissue culture incubator (Forma Scientific) with 5% CO₂. Iontophoresis injections and culture of embryos at perigastrulation stages (6.5 d.p.c.) were done as previously reported (Lawson et al., 1991; Faust et al., 1998).

Results

A morphologically distinct group of visceral endoderm cells covers portions of the epiblast at pregastrula stages

The chick hypoblast and anterior marginal crescent of rabbit embryos can be distinguished morphologically from other endodermal cells at pregastrula stages. In chick, the hypoblast can be distinguished from the endoblast, the posterior component of the endoderm, by its larger yolkier cells (Stern and Ireland, 1981; Bachvarova et al., 1998). In rabbit embryos, the anterior endoderm layer is composed of tall columnar cells that contrast with the more squamosal cells of the posterior portion of the embryonic disk (Viebahn et al., 1995). In mice, no morphological distinction was noted between AVE cells and the rest of the visceral endoderm (see review by Beddington and Robertson, 1999). However, a morphological distinction among cells of the embryonic visceral endoderm was suggested based on a retrospective analysis of published histological sections (Viebahn, 1999) and on whole-mount and histological observations of transgenic embryos (Kimura et al., 2000). In order to characterize the morphology of the visceral endoderm in whole-mount wild-type embryos, we analyzed embryos from the outbred mouse strain CD-1 immediately after dissection.

Embryos were collected between 11 and 19 h past midnight of the light cycle of the fifth day post-coitum. A total of 153 embryos from 14 litters were recovered. Of these, 75 nondamaged embryos were imaged and their morphology analyzed by using differential interference contrast microscopy. For each embryo, 3 measurements were obtained (Fig. 1A): egg cylinder length extending from the junction of the visceral and parietal endoderm to the tip of the cylinder (H); length of the embryonic portion of the egg cylinder, counting from the epiblast/extraembryonic ectoderm junction to the tip of the cylinder (h); and diameter of the embryonic portion of the egg cylinder, measured at the midlevel of the proamniotic cavity (d).

The majority of the embryos analyzed possessed a distinctive area of visceral endoderm thickening (VET) located along the proximodistal axis of the epiblast. Embryos were grouped in five categories according to visceral endoderm morphology: no VET and distal, laterodistal, lateral, and proximolateral VET location (Fig. 1B–G). Embryos with no VET were dissected at approximately 5.5 d.p.c. and averaged 125 μm in egg cylinder length (Fig. 2A). These embryos had an incipient proamniotic cavity and no obvious differences in visceral endoderm morphology (Fig. 1B). Embryos with a distally located VET (Fig. 1C) had an average egg cylinder length of 185 μm (Fig. 2A). The VET occupied only the distal tip of the embryo as evidenced by rotation of the egg cylinder about its proximodistal axis. The height of the VET epithelium at this position was at least twice that of the visceral endoderm covering lateral portions of the epiblast. In these embryos, the proamniotic cavity did not appear to extend into the extraembryonic ectoderm region. In the third group of embryos, the VET was positioned adjacent to the distal tip of the epiblast (Fig. 1D). Embryos with this laterodistal VET were slightly larger than embryos with a distal VET, averaging 207 μm egg cylinder length (Fig. 2A). The proamniotic cavity generally extended into the extraembryonic ectoderm region, and as in embryos with a distally located VET, the VET epithelium was approximately twice the height of the laterally located embryonic visceral endoderm.

Embryos with a lateral VET averaged 242 μm in egg cylinder length (Fig. 2A). The VET covered one side of the embryo spanning the entire length of the epiblast and approximately one-third of its circumference as evidenced by egg cylinder rotation (Fig. 1E and F). VET cells did not appear to extend over the extraembryonic ectoderm region. The proamniotic cavity in these embryos had expanded into the extraembryonic ectoderm. The largest embryos dissected had a less conspicuous VET generally most evident at the boundary between the epiblast/extraembryonic ectoderm regions (Fig. 1G). These embryos with a proximolateral VET location averaged 273 μm in egg cylinder length (Fig. 2A) and had a proamniotic cavity that extended well into the extraembryonic ectoderm region.

Analysis of embryo dimensions suggested a linear relationship between the embryonic length (h), embryonic width (d), and egg cylinder length (H) (Fig. 2). A simple regression analysis revealed that the embryonic length was equivalent to 51.29% ($h = 0.516H$, s.e. 0.0047, 95% CI: 0.517, 0.522) and the embryonic width to 52.21% ($d = 0.522H$, s.e. 0.052, 95% CI: 0.517, 0.537) of the egg cylinder length. The embryonic width was equivalent to 96.72% of the embryonic length ($d = 0.967h$, s.e. 0.0112, 95% CI: 0.945, 0.989).

The visceral endoderm thickening colocalizes with the expression of the Hex gene

The *Hex* gene has a dynamic pattern of expression restricted to the visceral endoderm before gastrulation commences (Thomas et al., 1998). In situ hybridization data show *Hex* expression at distal, laterodistal, and lateral positions of the visceral endoderm that covers the epiblast. This distal to proximal shift in *Hex* expression was observed within a period of 12 h between 5.5 and 6.0 d.p.c. Our morphological analysis suggested colocalization of the VET with the *Hex* expression domain and a distal-to-proximal shift of *Hex* expression within a period of approximately 6 h between 5.5 and 5.75 d.p.c. To analyze the spatiotemporal relationship between *Hex* expression and the VET, we used the random insertion transgenic line *Tg(Hex-eGFP)ARbe*. This line expresses the eGFP reporter gene under the control of the regulatory regions of the *Hex* gene (Rodriguez et al., 2001).

Twenty-two embryos heterozygous for the *Tg(Hex-eGFP)ARbe* transgene were analyzed for the *Hex*-eGFP fluorescence domain and VET location immediately after dissection. The *Hex*-eGFP fluorescence domain and the position of the VET colocalized in all the embryos analyzed regardless of VET position (Fig. 3), although not all the VET cells showed eGFP fluorescence (marked by an asterisk in Fig. 4F). Analysis of VET/*Hex*-eGFP fluorescence revealed a population of cells that formed a cap at the distal tip of the egg cylinder at about 5.5 d.p.c. (Fig. 3A and B). Laterodistal eGFP-positive cells formed a shield-like structure that extended proximally to about half the length of the epiblast and approximately one-third around the circumference of the epiblast (Fig. 3C–H). This area of VET/*Hex*-eGFP fluorescence reached the epiblast/extraembryonic ectoderm boundary in embryos with a lateral VET and covered approximately half of the circumference of the epiblast. *Hex*-eGFP fluorescent cells tended to align along the epiblast/extraembryonic ectoderm boundary; however, in some of the largest embryos analyzed, a few eGFP-positive cells were observed across the epiblast/extraembryonic ectoderm boundary overlying the extraembryonic ectoderm. These visceral endoderm cells did not spread more

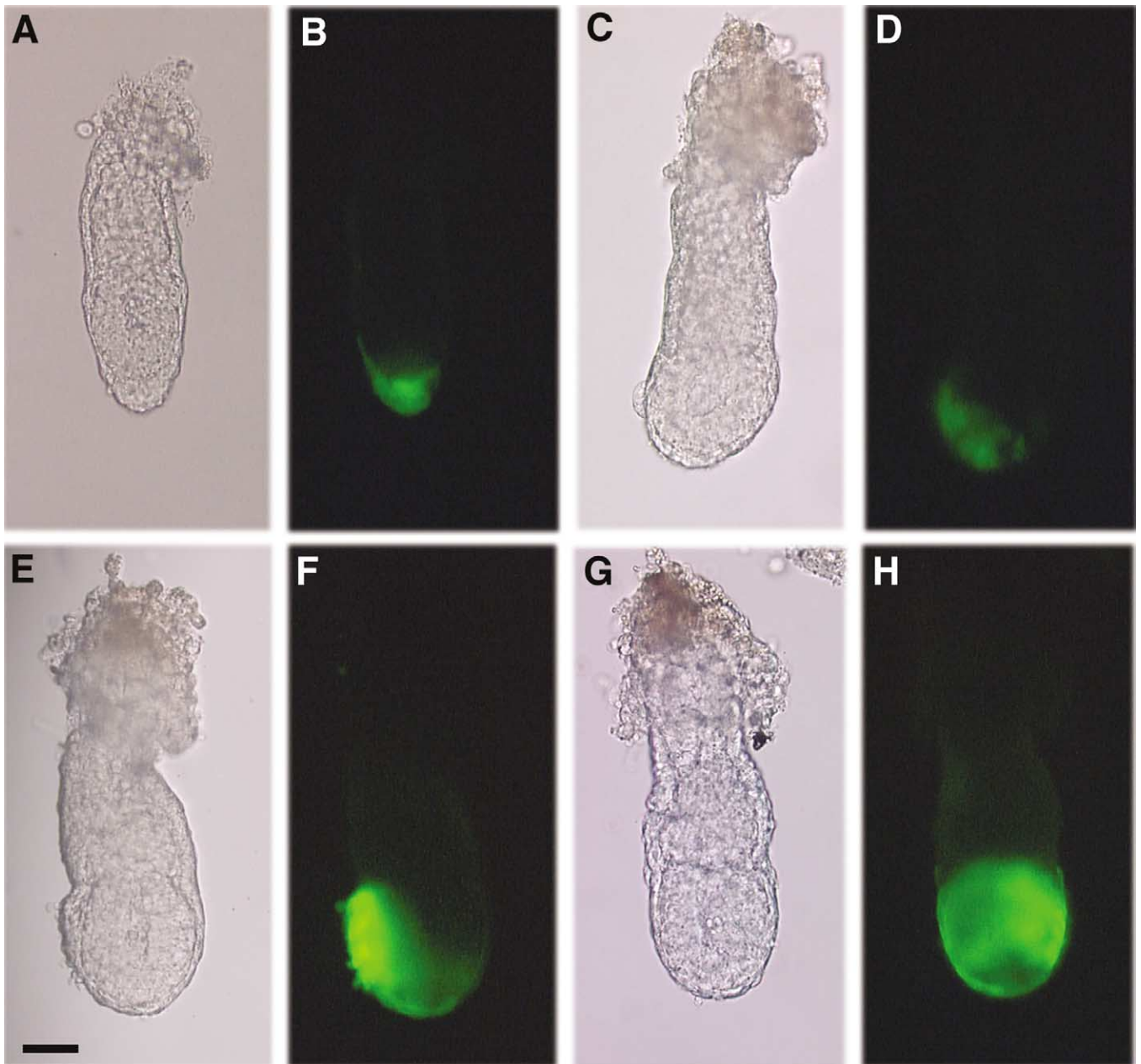
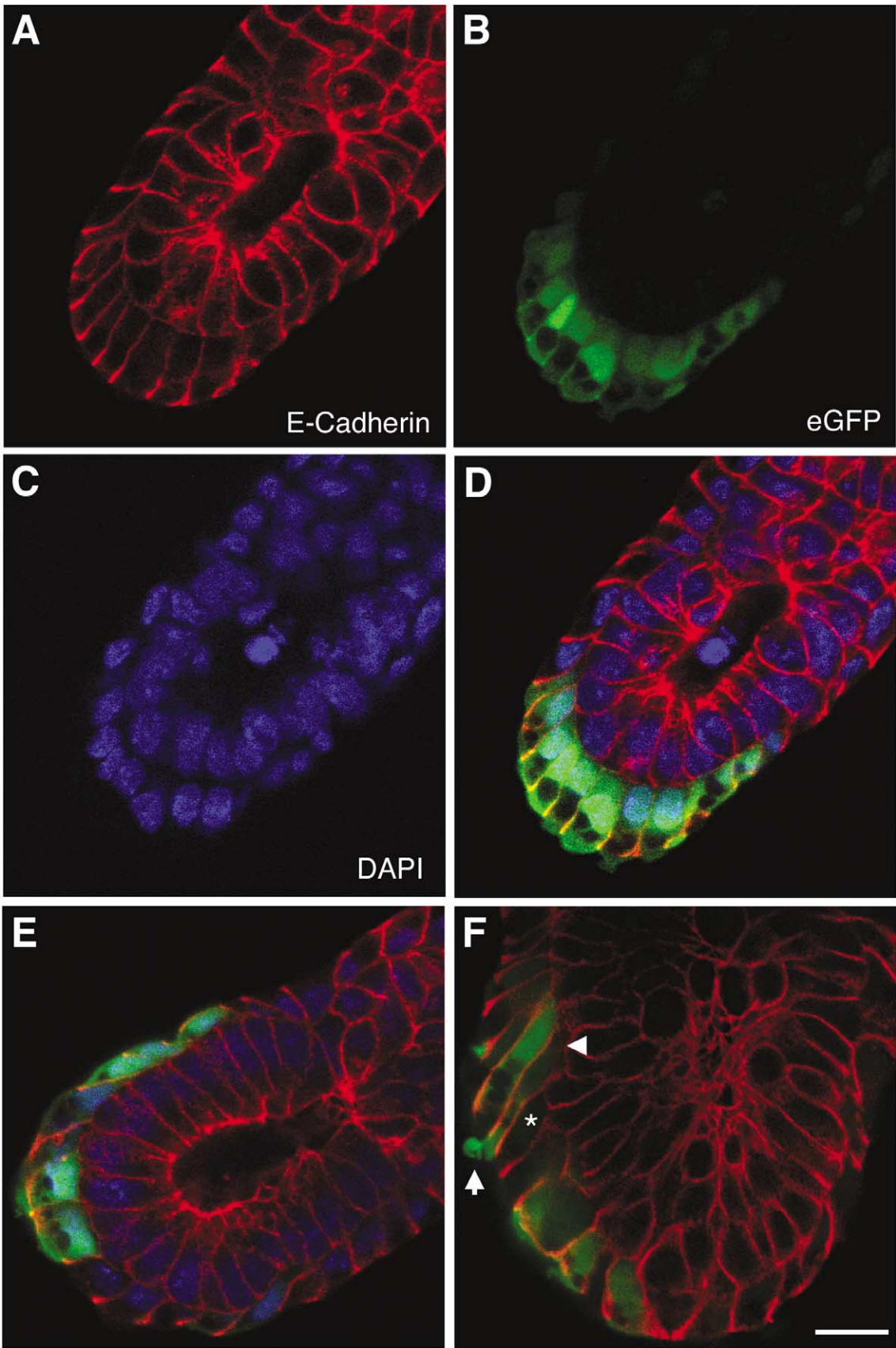


Fig. 3. The area of visceral endoderm thickening colocalizes with the expression of the *Hex* gene. Transmission (A, C, E, G) and fluorescence (B, D, F, H) illumination of embryos heterozygous for the *Tg(Hex-eGFP)ARbe* transgene. The areas of fluorescence colocalize with the area of visceral endoderm thickening in distal (A and B), laterodistal (C and D), and lateral (E–H) positions of the epiblast. (E–H) The same embryo in a side view (E and F) and after 90° rotation of the egg cylinder (G and H). All pictures are shown at the same magnification. Scale bar, 50 μm .

Fig. 4. The visceral endoderm thickening is a monolayer of tall columnar cells. Confocal microscope images of immunofluorescent pregastrulation embryos. Cell–cell contact surfaces are revealed with an anti-E-Cadherin antibody (A). The area of *Hex* expression is revealed by eGFP fluorescence produced by the *Tg(Hex-eGFP)ARbe* transgene (B) and the nuclei are stained with DAPI (C). (D and E) Merged pictures of the three staining patterns. (F) A merged figure of the eGFP and E-Cadherin fluorescence patterns. The VET is a simple columnar epithelium characterized by basal nuclei (D). VET cells are more columnar than other visceral endoderm cells and can be twice as tall (compare the eGFP positive VET cells and eGFP negative visceral endoderm cells in D). VET cells contain large vesicles that are evident as unstained areas at the apical region of the cytoplasm (see B, D, E, and F). Vesicles positive for eGFP are observed at the apical surface of VET cells (arrow in F). Some VET cells in embryos with laterodistal (E) and lateral VET (F) have a tilted orientation relative to the epiblast cells. Tilted cells are more evident in proximal regions of the VET and are oriented such that their basal surface points toward the proximal region of the egg cylinder (arrowhead in F). Some VET cells are negative for eGFP fluorescence (asterisk in F). All pictures are shown at the same magnification. Scale bar, 20 μm .



than one row of cells over the extraembryonic ectoderm (data not shown).

The visceral endoderm thickening is a monolayer of tall columnar cells

The bulging appearance of the VET prompted the question of whether this thickened area of visceral endoderm is produced by an increase in the height of single-layered epithelial cells, or alternatively, is the product of a multi-layered epithelial region. A previous study concluded that this area was a bilayer of pseudostratified columnar or stratified cuboidal epithelium based on analysis of semi-thin plastic sections from an *Otx2-LacZ* transgenic line (Kimura et al., 2000). In contrast to this report, however, direct observation of individual cells labeled with the fluorescent dye lysinated rhodamine dextran suggested a single-layered epithelium. VET cells were found to span the entire apical–basal extent of the visceral endoderm epithelium in distal ($n = 16$) laterodistal ($n = 7$), or lateral ($n = 10$) positions and in both wild type and *Tg(Hex-eGFP)ARbe* heterozygous embryos (not shown).

To confirm these observations, we conducted a whole-mount immunofluorescence analysis of the morphology of the visceral endoderm epithelium in embryos dissected between 5.5 and 5.75 d.p.c. *Tg(Hex-eGFP)ARbe* heterozygous embryos were stained with a rat monoclonal anti-E-cadherin antibody. This antibody recognizes adherent junctions and has been used to reveal cell–cell boundaries in early postimplantation embryos (Gallicano et al., 1998). Confocal optical sections of indirect immunofluorescence revealed by the anti-E-cadherin staining combined with DAPI nuclear staining showed no evidence of a stratified or pseudostratified visceral endoderm epithelium (Fig. 4). Analysis of serial sections of 14 embryos revealed that a single layer of visceral endoderm cells covered the egg cylinder. VET cells—revealed by eGFP fluorescence—were taller and more columnar than the rest of the visceral endoderm cells covering the epiblast (Fig. 4D). Cells in the VET also contained large vacuolae located at their apical region (Fig. 4D–F) and frequently contained vesicles associated with their apical surface (Fig. 4F). These characteristics gave VET cells a distinctive rugged surface appearance under DIC optics (not shown).

We also noted that VET cells occupying lateral positions of the epiblast frequently were slanted relative to the epiblast epithelium. Typically, cells showed a tilt of approximately 30–45° and were oriented in such a way that their basal surface pointed toward the epiblast/extraembryonic ectoderm boundary of the egg cylinder, while their apical surface pointed toward its distal tip (Fig. 4F). This characteristic cell orientation was also evident in 27 of 34 unlabeled embryos observed under DIC optics (not shown).

The epiblast of pregastrula embryos is bilaterally symmetric

Analysis of the embryos with the VET facing one side (side view) or facing up (upper view) suggested that the epiblast layer was a bilateral rather than a radially symmetrical structure (Fig. 5). In the majority of embryos with a laterodistal or lateral VET, the diameter of the epiblast appeared narrower in a side view than in an upper view. This difference in diameter gave the epiblast the appearance of a flattened sac-like structure (Fig. 5A). To test whether differences in epiblast dimensions were statistically significant, we measured the diameter of the epiblast at the midlevel of the proamniotic cavity in embryos with the VET facing one side and after 90° rotation (a and a' , respectively, Fig. 5B) and compared these measurements using Wilcoxon's signed rank test. To characterize the relationship between the two measurements, a simple linear regression was performed. The signed rank test supported a difference between the two measurements ($P = 0.0004$) (Fig. 5C). The regression analysis revealed that the diameter of the epiblast on a side view (a) corresponded to 97.21% of its diameter after 90° rotation (a') ($a = 0.9721a'$, s.e. = 0.0074, 95% CI: 0.9576, 0.9866). These results suggest that the epiblast is a bilateral structure and that its plane of symmetry (shorter diameter) bisects the VET. Similar measurements were taken of the egg cylinder at the same position (b and b' , Fig. 5B). The signed rank test supported a difference in the two measurements ($P = 0.0041$) (Fig. 5C); a simple regression analysis revealed that the diameter of the egg cylinder on a side view was larger than its diameter after 90° rotation. The side view diameter corresponded to 1.019 of the 90° rotated diameter ($b = 1.019b'$, s.e. 0.0057, 95% CI: 1.008, 1.030). The epiblast of embryos with a proximolateral VET, who were among the largest embryos dissected, appeared to have a cylindrical rather than a compressed morphology. These embryos, however, had a less conspicuous VET morphology that complicated the alignment of the egg cylinder to allow an accurate assessment of the epiblast morphology.

Distal tip visceral endoderm cells shift to proximal positions by 5.75 d.p.c.

The dynamic expression pattern of the *Hex* gene suggested that visceral endoderm cells at the distal tip of the egg cylinder were moving proximally toward the future anterior side of the embryo 24 h before the appearance of the primitive streak. To follow the movements of *Hex*-expressing cells, Thomas and coworkers (1998) labeled a group of visceral endoderm cells at the distal tip of the egg cylinder of 5.5 d.p.c. embryos with DiI and analyzed their distribution after a period of 24 h in culture. Descendants of labeled cells extended over a large area of the egg cylinder covering one side of the epiblast opposite to the primitive streak. These experiments demonstrated that distal visceral

endoderm cells undergo a proximal shift in their position toward the anterior portion of the embryo within a period of 1 day. Our morphological and fluorescence analysis of *Tg(Hex-eGFP)ARbe* embryos suggested that the distal-to-proximal shift of distal visceral endoderm cells had occurred by 5.75 d.p.c. Moreover, although the results of Dil labeling show a distal-to-proximal shift of the labeled cells, they do not address the movement of cells in specific regions within the labeled group. To follow the fate of distal VET cells, we labeled single cells with a mixture of horseradish peroxidase (HRP) and lysinated rhodamine dextran (LRDX) using iontophoresis (Lawson et al., 1991). The distribution of descendants of labeled cells was determined after a culture period of 6–9 h. Seventeen embryos with distal VET/eGFP fluorescence were labeled. Since embryos with a symmetrical distal VET did not provide information about the polarity of the embryo, we labeled embryos in which the VET was slightly tilted toward one side of the egg cylinder. These embryos were still at an earlier stage than embryos classified as laterodistal VET in which the VET/eGFP region extended to half the length of the proximodistal axis of the epiblast. Seven embryos were injected at the leading edge of the VET (Fig. 6A and B), five on a central location (not shown), and five at the trailing edge of the VET (Fig. 6C). One cell was impaled at each injection, although sometimes more than one cell was unintentionally labeled due to diffusion of the label between sister cells across cytoplasmic bridges. After the culture period, 16 embryos had the VET/eGFP fluorescence reaching the epiblast/extraembryonic ectoderm boundary or were within 1 or 2 cell diameters from it (not shown). One of the embryos was abnormal remaining small and with eGFP fluorescence at a distal position. In all 16 normal embryos, the labeled cells had shifted from a distal to a proximal position of the epiblast and formed both coherent and not coherent clones. Descendants of cells labeled at the leading edge or central portions of the VET were generally located at more proximal positions than descendants of cells at the trailing edge of the VET (data summarized in Fig. 7). The majority of labeled embryos showed diagonally (Fig. 6A, 9/16 cases) or horizontally (Fig. 6B, 3/16 cases) arranged areas of HRP staining relative to the proximodistal axis of the egg cylinder. Only in one case did we observed a proximodistally aligned clone with the remaining 3 embryos showing cir-

cular patterns of staining. These results suggest a distal-to-proximal shift of VET/*Hex*-expressing cells over a period spanning 5.5 and 5.75 d.p.c.

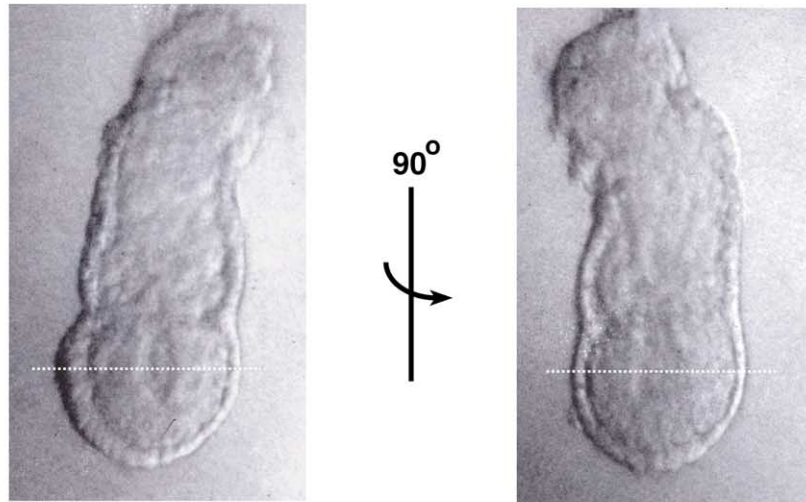
Lineage analysis of VET cells from prestreak to perigastrulation stages

Dil lineage experiments suggested that distal tip visceral endoderm cells move proximally as a coherent population, ending in the anterior portion of the embryos by primitive streak stages (Thomas et al., 1998). We attempted to follow the fate of distal tip VET cells to primitive streak stages; however, distal VET (5.5 d.p.c.) embryos cultured for 24 h had a tendency to develop an abnormally distended proamniotic cavity that in some cases did not expand into the extraembryonic ectoderm region (data not shown). To overcome this disadvantage, we decided to follow the fate of distal VET cells after they had shifted to one side of the embryo at about 5.75 d.p.c. (Fig. 8; summarized in Table 1). The majority of the 5.75 d.p.c. embryos developed normally after approximately 24 h in culture as judged by the development of the primitive streak (12/15 embryos); however, some embryos developed an expanded proamniotic cavity. Nonetheless, the majority of 5.75 d.p.c. embryos cultured for 48 h developed an amnion, node, and headfolds (not shown).

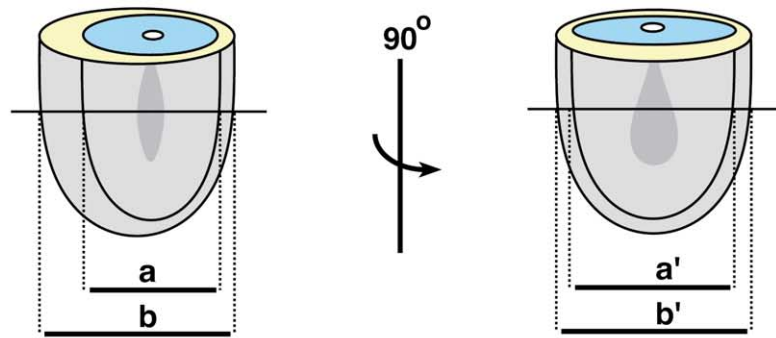
VET cells were labeled in locations along the proximodistal axis of the epiblast and the embryos cultured to primitive streak stages. Eight embryos were labeled at the anterior–proximal third of the VET region (Fig. 8A). In six of these embryos that developed a primitive streak, descendants of labeled cells were distributed in regions located close to the epiblast/extraembryonic ectoderm boundary with some cells in the extraembryonic region. Labeled cells produced short segments or stripes of HRP stained cells that tended to form an arc oriented from anteroproximal to lateral positions of the epiblast. Fig. 8A shows an early streak embryo with two short segments of HRP-positive cells located on a lateral position. These cells straddle the epiblast/extraembryonic ectoderm boundary. Similar results were obtained when VET cells located closer to the distal tip of the embryo were labeled (not shown). Six labeled embryos cultured to primitive streak stages contained segments or stripes of cells located over anteroproximal regions

Fig. 5. The epiblast of pregastrula embryos is compressed anteroposteriorly. (A) Images of an embryo pictured with the VET facing one side and after the embryo was rotated 90°. The epiblast layer has a compressed shape that is evident after rotation of the embryo. The difference in epiblast width is not reflected in the dimensions of the embryonic portion of the egg cylinder at the same level instead and increase in the thickness of the visceral endoderm on one side of the epiblast compensates for this compression. (B) Diagram illustrating the differences in epiblast morphology at the midlevel of the proamniotic cavity (dotted line in A). *a* and *a'* represent the diameter of the epiblast in a side view and after 90° rotation of the egg cylinder, respectively. *b* and *b'* represent the diameter of the egg cylinder. (C) Scatter plot depiction of the differences obtained from a comparison between the diameter of the epiblast and egg cylinder in a side view and after 90° rotation. A comparison between the epiblast width (*a'*–*a*) is shown in the upper panel and that of the egg cylinder diameter (*b'*–*b*) in the lower panel. Embryos with a laterodistal VET are shown in green (*n* = 27) and embryos with lateral VET in blue (*n* = 28). The diameter of the epiblast on a side view is smaller than its diameter measured after 90° rotation (Wilcoxon's paired test, *P* = 0.0004). A simple regression analysis reveals that *a* = 0.9721*a'* (s.e. 0.0074, 95% CI: 0.9576, 0.9866). The diameter of the egg cylinder is larger in a side view than after rotation of the egg cylinder (Wilcoxon's paired test, *P* = 0.0041). A simple regression analysis shows that *b* = 1.019*b'* (s.e. 0.0057, 95% CI: 1.008, 1.030).

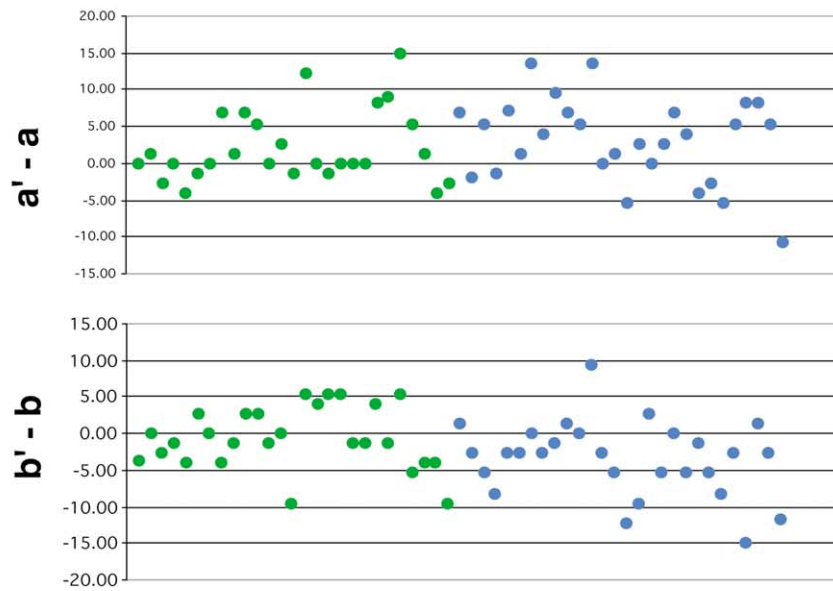
A



B



C



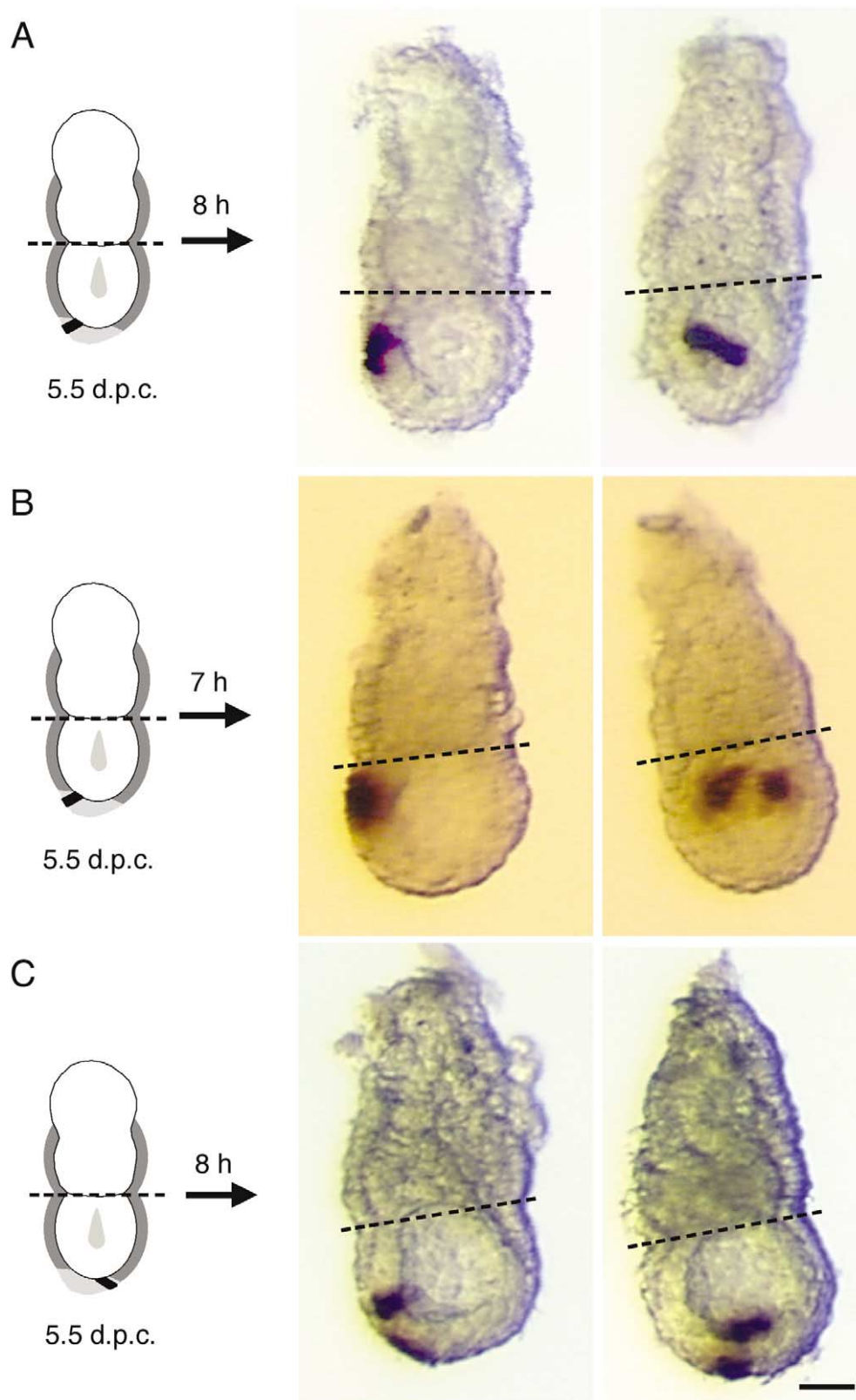


Fig. 6. Lineage analysis of VET/*Hex*-expressing cells located at the distal tip of the egg cylinder. Visceral endoderm cells of *Tg(Hex-eGFP)ARbe* embryos with distal VET dissected at about 5.5 d.p.c. were labeled iontophoretically. To follow the movements of cells in different regions of the VET, embryos in which the distal VET/eGFP fluorescence had a slight tilt toward one side of the embryo to position the labeling site were used. Cells were labeled at the leading edge (most proximal position of VET/eGFP fluorescence) (A and B), central position (not shown), or trailing edge (C) of the VET. After culture for a period of 6–9 h, descendants of the labeled cells had shifted from distal-to-proximal positions in all embryos analyzed (see Fig. 7 for summary). The areas of HRP staining tended to spread mainly in diagonal (A and C, 9/16 cases) or horizontal (B, 3/16 cases) planes relative to the proximodistal axis of the egg cylinder. Only one cell was impaled at the time of injection, but more cells may have been labeled unintentionally. Embryo pictures are shown in a side view (left) and after 90° rotation (right). All pictures shown at the same magnification. Scale bar, 40 μ m. The dashed line demarcates the epiblast/extraembryonic ectoderm boundary.




Injection Site	Embryo No.	No. Injected Cells	Proximo-Distal Location of Descendants Along Epiblast Surface		
			Prox. Tier	Middle Tier	Distal Tier
	1	1		+++	+
	2	2	+	+++	
	3	1		++	++
	4	2	++	++	
	5	1	++++		
	6	2	+++	+	
	1	3	+	++	+
	2	1 or 2	+	+++	
	3	2	+++	+	
	4	1	+	+++	
	5	1	+	++	+
	1	2		++++	
	2	1 or 2	+	+++	
	3	1 or 2		++++	
	4	2		++	++
	5	2			++++

Fig. 7. Distribution of descendants of distal VET cells along the proximo-distal axis of the epiblast at 5.75 d.p.c. The position of descendants of labeled cells at the leading (upper section), central (middle section), or trailing edge (lower section) of the VET was determined according to the distribution of the HRP positive area along the proximal, central, or distal tiers of the epiblast. Cells at the leading or central positions of the VET tended to occupy more proximal positions of the epiblast surface than cells in the trailing edge. The (+) sign represents approximately one-quarter of the total HRP-stained area.

of the epiblast or laterally. The overall pattern of cell distribution appeared to delineate the anterior half of the embryo. The embryo in Fig. 8B illustrates this pattern of cell distribution. In this prestreak embryo, three labeled VET cells at the anterior mid-epiblast position produced a well-defined arc that extended from an anteroproximal to a mid-lateral position of the egg cylinder. These results together with the analysis of distal VET cells, suggest an antero and anterolateral movement of VET cells rather than a distal-to-proximal vectorial movement of along the anterior mid-line of the embryo.

An endoblast-like visceral endoderm cell population

Lineage studies using chick embryos have shown that the endoblast, an extraembryonic population of cells, displaces the hypoblast—a *Hex*-positive cell population—anteriorly (Foley et al., 2000, and references herein). To determine whether there was an endoblast-like cell population in mouse embryos, we labeled distal tip visceral endoderm (non-VET/*Hex*) cells in embryos with a lateral VET (Fig. 8C). We cultured these embryos to pregastrulation stages to assess the position of distal visceral endoderm before the appearance of the definitive endoderm cells derived from the primitive streak. To mark the position of the VET in prestreak wild-type embryos, an extraembryonic visceral endoderm cell was labeled proximal to the epiblast/extraembryonic ectoderm junction of the egg cylinder (arrowhead in Fig. 8C). This extraembryonic label was placed in direct

alignment with the lateral VET. Previous experiments, in which single extraembryonic visceral endoderm cells were labeled, showed that descendants of these cells remain coherent and mark the anterior side of the embryo since their descendants are found opposite to the primitive streak (data not shown).

A total of 19 embryos were labeled and cultured for 14–19 h. In 12 of these embryos, distal cells shifted anteriorly in the direction of the VET. Six embryos did not contain labeled cells or developed abnormally (see Table 1). Clonal descendants were located in proximal and middle regions of the epiblast and tended to spread over the anterior half of the embryo (Fig. 8C). Also, they remained close to each other but were not strictly coherent. The extraembryonic visceral endoderm clone formed a coherent patch (arrowhead in Fig. 8C). One embryo cultured for 24 h developed to early primitive streak stage. In this embryo, noncoherent descendants of the labeled distal visceral endoderm cells were found opposite to the primitive streak distributed along proximal and midanterior epiblast regions in a similar manner to embryos at preprimitive streak stages (not shown). These results suggest that a population of endoblast-like visceral endoderm cells displaces VET descendants anteriorly and that the shift in cell position begins before the primitive streak is morphologically distinguishable.

Lineage analysis of proximoanterior AVE cells at perigastrulation stages

Our lineage analysis indicated that descendants of distal VET cells formed a crescent extending from anteroproximal regions to midlateral positions of the egg cylinder at primitive streak stages. A lineage analysis of visceral endoderm cells at perigastrulation stages has shown that visceral endoderm cells at the anterior half of the axis are displaced anteriorly and anterolaterally and are found in the visceral yolk sac after 2 days in culture (Lawson and Pedersen, 1987). To follow the fate of proximoanterior VET/AVE cells, we labeled embryos at prestreak ($n = 5$) and early streak stages ($n = 4$) and cultured them for approximately 1 day (Fig. 9). Our results support the previous report of Lawson and Pedersen (1987). Labeled cells produced short stripes of HRP-positive cells in the extraembryonic region that tended to form an arc around the cranial end of the embryo (Fig. 9).

Analysis of the eGFP fluorescence provided by the *Tg(Hex-eGFP)ARbe* transgene suggested that descendants of the proximal AVE abut definitive endoderm cells at headfold stages. HRP-positive cells were negative for eGFP fluorescence and bordered the anterior definitive endoderm indicated by the eGFP fluorescence provided by the transgene (Rodriguez et al., 2000).

Table 1
Summary of lineage analysis of 5.75 and 6.5 d.p.c. embryos

Stage	Location label	Total injected (abnormal)	Culture time (h)	Embryos with labeled cells	D & D developmental stage ^a						
					PS	ES	MS	LS	LB	EHF	LHF
Lateral VET (~E5.75)	Antero-Prox. VET	8 (1)	24–26	7	1	6	—	—	—	—	—
Lateral VET (~E5.75)	Antero-Distal VET	7 (1)	25–27	5	—	—	5	1	—	—	—
Lateral VET (~E5.75)	Distal Visc. End.	19 (4)	14–19	12	12	—	—	—	—	—	—
Lateral VET (~E5.75)	Distal Visc. End.	1	24	1	—	1	—	—	—	—	—
Pre—Streak (~E6.5)	Antero—Prox. AVE	5	24–27	5	—	—	—	—	5	—	—
Early Streak (~E6.5)	Antero—Prox. AVE	5	24–27	5	—	—	—	—	—	3	1

Note. One early streak embryo showed an abnormal punctuated staining and was excluded from the analysis.

^a Downs and Davies (1993).

Discussion

Morphological asymmetries in visceral endoderm signal the future anteroposterior axis of the mouse embryo at pregastrulation stages

Traditionally, the visceral endoderm has been divided morphologically into two populations of cells: tall columnar cells that cover the extraembryonic ectoderm and flat squamous cells that cover the epiblast (Batten and Haar, 1979). However, this morphological distinction corresponds to embryos at the onset of gastrulation at approximately 6.5 d.p.c. In this study, we describe a distinctive thickened area of visceral endoderm (VET) that overlies different portions of the epiblast at preprimitive streak stages. Direct observations of fluorescently labeled cells and analysis of optical sections of immunofluorescent embryos demonstrate that VET cells span the entire thickness of the epithelium and contact the basal membrane. Thus, the VET is a monolayer of tall columnar epithelial cells. These cells are characterized by the presence of larger apical vacuolae and surface vesicles that give it a rugged appearance that is distinct of other visceral endoderm cells and can be distinguished under DIC optics. Analysis of the transgenic line *Tg(Hex-eGFP)ARbe* revealed that the expression of the *Hex* gene and the region of visceral endoderm thickening colocalize. The expression of *Hex* marks the anterior portion of the embryo at pregastrulation stages. Therefore, the VET serves as a morphological marker of the anteroposterior axis of the preprimitive streak embryo.

Kimura and colleagues (2000) described a region of visceral endoderm thickening marked by the expression of an *Otx2-eGFP* transgene at the distal portion of the epiblast. Our analysis confirms these observations using wild type embryos and heterozygous *Tg(Hex-eGFP)ARbe* embryos. In addition, we find that the thickened region is more extensive than previously described, reaching the epiblast/extraembryonic ectoderm boundary in later stages. The same authors also reported that the thickened region was a

bilayered pseudostratified or cuboidal epithelium. Our results show that the VET is a simple columnar epithelium. A possible explanation for this discrepancy is that Kimura and coworkers based their conclusions on analysis of transverse sections of the egg cylinder. During our study, we noticed that VET cells have a slanted orientation when they are located on one side of the epiblast; therefore, it is possible that their sections show a monolayer of slanted VET cells that give the appearance of a multilayered epithelium in a cross section.

Studies of pregastrula mouse embryos have been hampered in part by the lack of the staging system. The asymmetries observed in the visceral endoderm of the preprimitive streak embryos offer morphological landmarks to stage mouse embryos. These landmarks coupled with the use of fluorescent transgenic lines like *Tg(Hex-eGFP)ARbe* provide invaluable tools for future embryological studies of preprimitive streak embryos.

The epiblast of pregastrulation embryos is compressed anteroposteriorly

Using the VET as a landmark to orient the embryos, we noticed that the epiblast is compressed anteroposteriorly. Hence, the epiblast layer is not a radially symmetric structure but a bilateral structure whose plane of symmetry (shorter diameter) bisects the VET. To our knowledge, this is the first time this characteristic of pregastrulation embryos has been described. In rabbit embryos, an increase in the height of the epiblast epithelium is associated with an increase in the height of the endoderm at the anterior marginal crescent of the blastodisc (Viebahn et al., 1995). We have not observed differences in the height of the epiblast at the stages studied; however, the compressed morphology of the epiblast coincided with the increase in the height of the visceral endoderm epithelium on one side of the embryo. These results suggest a link between the changes in visceral endoderm and epiblast morphology in both species of mam-

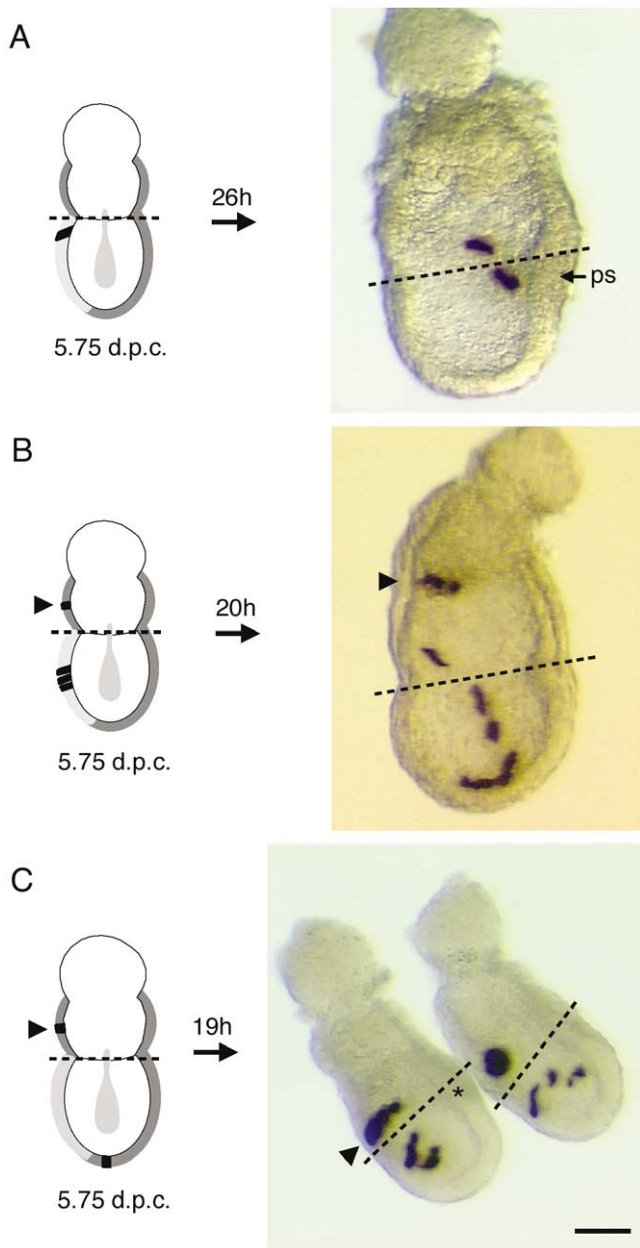


Fig. 8. Lineage analysis of visceral endoderm cells in 5.75 d.p.c. embryos. Visceral endoderm cells located along the proximodistal axis of the epiblast were labeled iontophoretically and the location of their descendants determined at perigastrulation stages. (A) Distribution of descendants of VET cells from the anteroproximal region. (B) Descendants of anterior middle VET cells; and (C) of distal non-VET visceral endoderm cells at preprimitive streak stage. Descendants of VET cells formed short segments (A, B) or stripes of HRP-positive-cells located over anterior (not shown) or lateral positions of the egg cylinder. The overall pattern of HRP staining suggested a crescent shaped distribution that delineated the anterior half of the epiblast extending from regions proximal to the epiblast/extraembryonic ectoderm boundary anteriorly to midlateral regions of the epiblast at early primitive streak stage. Descendants of the distal visceral endoderm cells (non-VET/eGFP fluorescence) produced noncoherent clones located in mid-anterior positions of the epiblast (C). Arrowheads in (B) and (C) indicate descendants of visceral endoderm cells from anterior regions of the embryo proximal to the epiblast/extraembryonic ectoderm boundary. These cells do not change position during embryo development and therefore mark the

malis at stages predating the appearance of the primitive streak.

Positional shift and distribution pattern of Hex-expressing visceral endoderm cells

A lineage analysis using Dil to follow distal visceral endoderm cells of 5.5 d.p.c embryos over a period of 24 h suggested that *Hex*-expressing cells shifted proximally to the anterior epiblast by primitive streak stages (Thomas et al., 1998). Our lineage analysis of distal VET cells together with morphological and fluorescence analysis of the transgenic line *Tg(Hex-eGFP)ARbe* indicate that distal VET/*Hex*-expressing cells occupy the anterior side of the epiblast by 5.75 d.p.c., 18 h before the appearance of the primitive streak. In the same study, distal tip visceral endoderm cells of 5.5 d.p.c. embryos are reported to move proximally as a coherent population to the future anterior side of the embryo. Our lineage study using iontophoresis revealed an antero and anterolateral spread of distal VET/*Hex*-expressing cells that culminated with their location at the boundary separating embryonic and extraembryonic tissues at head-fold stages. These results indicated that descendants of VET/*Hex*-expressing cells form a crescent over the anterior portion of the embryo at primitive streak stages rather than a coherent patch as suggested by Dil experiments (Thomas et al., 1998). Fig. 10 illustrates a proposed model that describes the shift in the position of VET/*Hex*-expressing cells. The differences in the distribution of distal visceral endoderm cells obtained could be a consequence of the lineage technique used. Dil labeling monitors the behavior of groups of cells while iontophoresis allows an analysis of individual cells, thus permitting a finer analysis of cell movements. The failure to distinguish between VET/*Hex*-expressing and non-VET/*Hex*-expressing visceral endoderm cell can also complicate the analysis of preprimitive streak embryos using Dil. As shown in these study, non-VET/*Hex* cells occupy the distal tip of the egg cylinder at prestreak stages and shift to the anterior portion of the embryo by primitive streak stages.

Analysis of individual VET cells revealed a slanted orientation relative to epiblast cells in embryos with a lateral VET. The basal surface of the cells was closer to the epiblast/extraembryonic ectoderm junction of the embryo than their apical surface. The slanted cell orientation suggests an active migration of distal cells over the surface of the epiblast such that the base of the epithelium advances

anterior portion of the embryo. (A, B) The right side of the embryo is shown, the images have been flipped horizontally to maintain a consistent embryo orientation. The asterisk marks the position of a thickening of the epiblast that precedes the formation of the primitive streak. The dashed line demarcates the epiblast/extraembryonic ectoderm boundary. Embryos in (A) and (B) shown at the same magnification. Scale bar, 80 μ m (A), (B) and 100 μ m (C). ps, primitive streak.

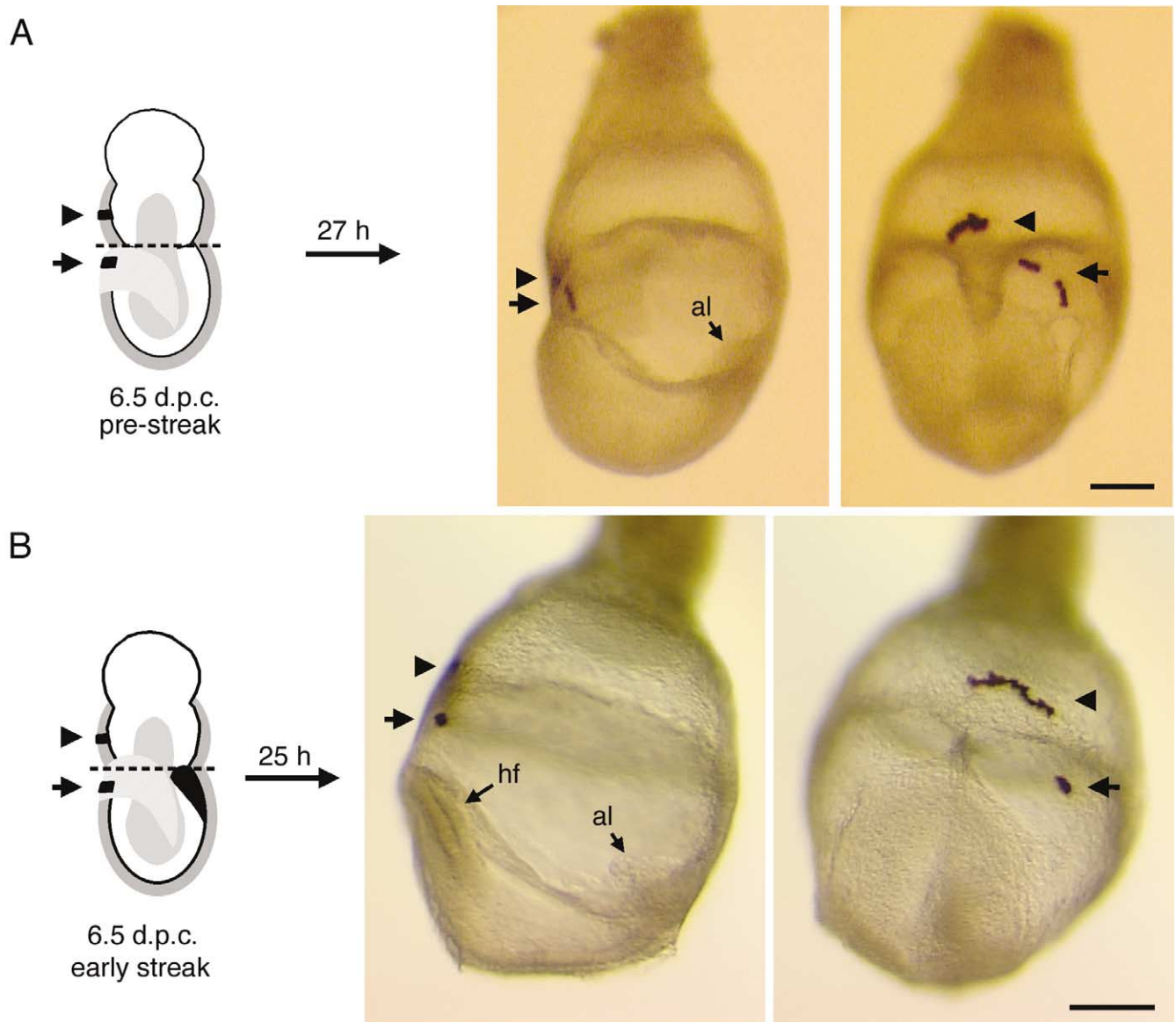


Fig. 9. Lineage analysis of proximal AVE cells in 6.5 d.p.c. embryos. Proximal AVE cells were labeled in prestreak (A) and early streak (B) embryos. Descendants of labeled cells formed short segments of HRP-stained cells located in anterolateral positions of the visceral yolk sac (arrows) after approximately 24 h in culture. Embryo pictures are shown in a side (left) and frontal view (right). Arrowhead points to clones derived from one (A) or three (B) extraembryonic visceral endoderm cells used to mark the anterior position of the embryo at the time of labeling (Lawson et al., 1991). In prestreak embryos, fluorescence provided by the *Tg(Hex-eGFP)ARbe* transgene was used to orient the embryos. Side view pictures show the right side of the embryos; the images have been flipped horizontally to maintain a consistent embryo orientation. Scale bar, 150 μ m in (A) and 200 μ m in (B). al, allantois; hf, headfolds.

ahead of its apical surface. The proximal shift of distal visceral endoderm cells could also be a consequence of cellular events happening in the epiblast component of the egg cylinder or a combination of events happening in both layers of the embryo. In embryos mutant for the gene *Cripto*, the distal visceral endoderm cells do not shift to a proximal position (Ding et al., 1998). *Cripto* is not expressed in the visceral endoderm or its precursors (Dono et al., 1993; Ding et al., 1998); therefore, the proximal shift of distal visceral endoderm cells requires the proper function of epiblast.

Extra-embryonic endoderm and anterior neural development

The signals that direct anterior neural development in mice are believed to emanate from the AVE and from derivatives of the node (Beddington and Robertson, 1998; Shawlot et al., 1999; Tam and Steiner, 1999). The role of the AVE in rostral signaling is supported by chimera experiments in which the visceral endoderm is derived from cells mutant for genes with axial defects like *nodal*, *Otx2*, *Hnf3 β* , and *Lim1* (Varlet et al., 1997; Rhin et al., 1998;

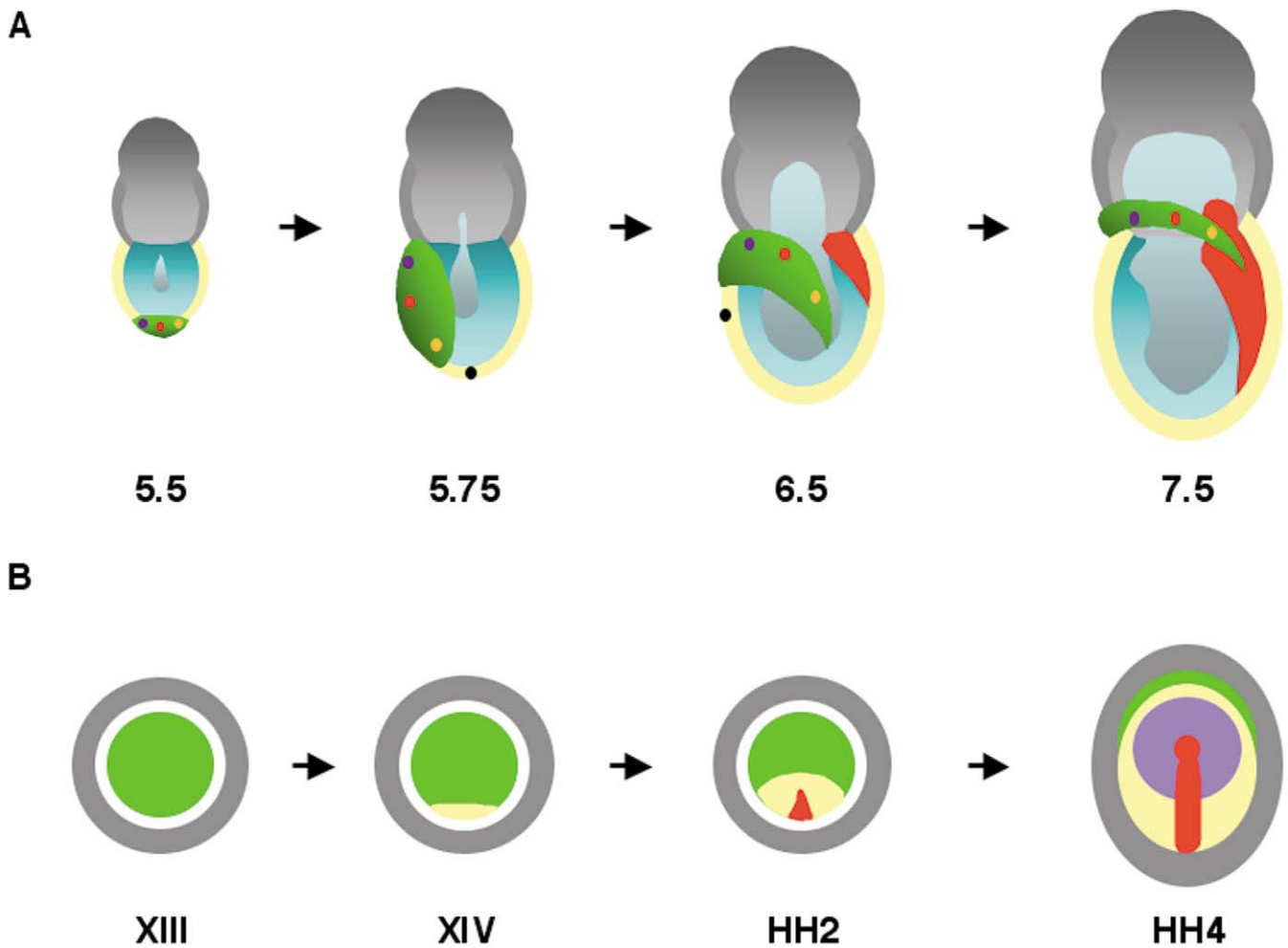


Fig. 10. Model depicting the positional shift of distal visceral endoderm cells from 5.5 to 7.5 d.p.c. and comparison to the fate map of the chick embryo. (A) VET/*Hex*-expressing cells (shown in green) form a shield of tall columnar epithelium at the distal tip of the egg cylinder at approximately 5.5 d.p.c. These cells shift to the anterior side of the epiblast by 5.75 d.p.c. At primitive streak stages, at approximately 6.5 d.p.c., VET descendants form a crescent that extends from regions proximal to the anterior epiblast/extraembryonic ectoderm boundary to midlateral regions of both sides of the epiblast. By headfold stages, at 7.5 d.p.c., crescent cells are distributed along the cranial boundary between the visceral yolk sac endoderm and the definitive endoderm. VET/*Hex*-expressing cells appear to spread anteriorly and anterolaterally (see dots) and are replaced by non-VET/*Hex*-expressing visceral endoderm (black dot). (B) Diagram depicting the hypoblast, endoblast, and definitive endoderm movements in chick embryos from E-G & K stage XIII to HH stage 4. The overall pattern of extraembryonic endodermal cell distribution in the two species is conserved despite the differences between the cylindrical mouse and the flat chick embryo. Mouse: green; VET, yellow; non-VET visceral endoderm; and blue, epiblast. The ectoplacental cone extraembryonic ectoderm and overlying visceral endoderm and yolk sac of 7.5 d.p.c. embryos are shown in gray. Chick: green, hypoblast; yellow, endoblast; white, marginal zone; purple, definitive endoderm; and gray, area opaca. The primitive streak in both embryos is shown in red. The extent of endoblast-like visceral endoderm and definitive endoderm in the mouse embryo is not depicted. The chick embryo diagrams are based on Eyal-Giladi and Kochav (1976) and Foley et al. (2000).

Duffort et al., 1998; Shawlot et al., 1999). It is puzzling, however, that ablation, grafting, or explant recombination experiments in mice have failed to demonstrate conclusively a neural inductive role for the AVE. Ablation of the AVE led to truncations of the prosencephalon suggesting an inductive role for this tissue (Thomas and Beddington, 1996). These experiments, however, cannot distinguish between an inductive or a trophic effect (Beddington and Robertson, 1998). The AVE has also failed to induce neural markers when grafted into the flank of late-streak embryos (Tam and Steiner, 1999) or in tissue recombination experiments (Kimura et al., 2000). In grafting experiment using

rabbit embryos as donors, the endoderm from the preprimitive streak anterior marginal crescent but not from the mid-streak anterior visceral endoderm induced neural markers (Knoetgen et al., 1999). The embryological experiments done in mice were performed at early streak stages; therefore, it is possible that the failure to detect neural inductive signals in the AVE was due to differences in the developmental stage of the embryos used as donors. Moreover, due to the shift in the position of the VET/*Hex*-expressing cells and the lack of markers, it is possible that non-VET/*Hex*-expressing cells were used. Our lineage analysis at stages preceding gastrulation and lineage analysis of visceral

endoderm cells at stages immediately before the appearance of the primitive streak show similar anterolateral cell shifting patterns (Lawson and Pedersen, 1987). These results indicate that the anterior visceral endoderm of 5.75 d.p.c. embryos and that of embryos at primitive streak stages are composed of different cell populations. The anterior epiblast half of embryos at 5.75 d.p.c. is covered by VET/*Hex* cells, while the same region of early streak stage embryos contains descendants of VET/*Hex* cells in anteroproximal and lateral regions while the rest is covered by non-VET visceral endoderm cells (see model on Fig. 10). The morphological and fluorescent landmarks described here provide the necessary tools to explore the neural inductive activities of specific regions of visceral endoderm at pre-primitive streak stages.

Evolutionary conservation of the pregastrula endodermal component of vertebrates

In chick and rabbit embryos, two populations of extraembryonic endoderm underlie the epiblast before gastrulation begins. In chick, the hypoblast can be distinguished from the posterior endoblast by the expression of several genes like *Hex*, *Gooseoid*, *Otx2*, and *cCer* (Foley et al., 2000). Morphologically, the hypoblast can also be distinguished from the endoblast by its larger cells and yolker cytoplasm (Stern and Ireland, 1981; Bachvarova et al., 1998). In rabbit embryos, the anterior endoderm as well as its overlying epiblast, are characterized by increased cellular height and number (Viebahn et al., 1995). Furthermore, histological analyses suggest that anterior embryonic differentiation, similar to that in the rabbit is present in other mammals like mouse, cat, bat, and primates including humans (reviewed by Viebahn, 1999).

Based on topology, expression pattern of several genes, and Dil analysis of distal visceral endoderm cells, the AVE was equated to the hypoblast of the chick (Beddington and Robertson, 1998). Our analysis suggests that VET/*Hex*-expressing visceral endoderm cells are equivalent to the hypoblast based on topological, morphological, and pattern of cell distribution at pre- and postgastrulation stages. Furthermore, based on cell movements, a population of distal non-VET/*Hex*-expressing cells of 5.75 d.p.c. embryos appear to be equivalent to the chick endoblast. The VET seems to be equivalent to the endodermal layer of the anterior marginal crescent of the rabbit (Viebahn et al., 1995). As in rabbit embryos, the mouse lateral VET cells are taller than visceral endodermal cells covering the opposite side of the epiblast (Viebahn, 1995).

Based on expression of the *Hex* gene, the AVE has been proposed to reside in yolk cells at the center of the blastocoel floor of *Xenopus* that move to the dorsal side of the embryo as gastrulation commences (Jones et al., 1999). In zebrafish, the cognate of *Hex* suggests equivalence between the dorsal yolk syncytial layer and the AVE (Ho et al.,

1999). A comparison of endodermal and ectodermal components between amphibians and amniotes with large yolk contents have led to the proposal that the hypoblast is an evolutionary derivative of the endodermal wedge already present in amphibians (Arendt and Nübler-Jung, 1999). The endodermal wedge is a mass of deep endodermal cells that slide upwards along the inner surface of the blastocoel roof towards the animal pole (Arendt and Nübler-Jung, 1999). The term “hypoboly” has been coined to describe *the active spreading of the deep endodermal cells along the inner surface of the blastocoel roof towards the animal pole* (Arendt and Nübler-Jung, 1999). Hypoboly is a movement of cells opposite to epiboly and both have in common the sliding against each other of endodermal and ectodermal cells (Arendt and Nübler-Jung, 1999). An analysis of the relative movements of the visceral endoderm and epiblast layers will determine whether a similar relationship among the two layers of cells exist in mice.

Acknowledgments

We thank Tristan Rodriguez and the late Rosa Beddington for kindly providing us with *Tg(Hex-eGFP)ARbe* transgenic mice. Iontophoretic injections could not have been done without the help of Cindy Faust. We thank Jacqueline Johnson and Michael Schell for help with the statistical analysis and Tim Oliver for help with confocal microscopy. Beth Morin-Kensicki provided insightful comments on the manuscript. J.A.R-P. was supported by a postdoctoral fellowship from the American Heart Association. This work was supported by NIH and March of Dimes grants (to T.M.).

References

- Arendt, D., Nübler-Jung, K., 1999. Rearranging gastrulation in the name of yolk: evolution of gastrulation in yolk-rich amniote eggs. *Mech. Dev.* 81, 3–22.
- Bachvarova, R.F., Skromne, I., Stern, C.D., 1998. Induction of primitive streak and Hensen's node by the posterior marginal zone in the early chick embryo. *Development* 125, 3521–3534.
- Batten, B.E., Haar, J.L., 1979. Fine structural differentiation of germ layers in the mouse at the time of mesoderm formation. *Anat. Rec.* 194, 125–142.
- Beddington, R.S.P., 1994. Induction of a second neural axis-by the mouse node. *Development* 120, 613–620.
- Beddington, R.S.P., Robertson, E.J., 1998. Anterior patterning in the mouse. *Trends Genet.* 14, 277–284.
- Beddington, R.S.P., Robertson, E.J., 1999. Axis development and early asymmetry in mammals. *Cell* 96, 195–209.
- Ding, J., Yang, L., Yan, Y.-T., Chen, A., Desai, N., Wynshaw-Boris, A., Shen, M.M., 1998. *Cripto* is required for correct orientation of the anterior-posterior axis in the mouse embryo. *Nature* 395, 702–707.
- Dono, R., Scalera, L., Pacifico, F., Acampora, D., Persico, M.G., Simeone, A., 1993. The murine *cripto* gene: expression during mesoderm induction and early heart morphogenesis. *Development* 118, 1157–1168.

- Downs, K.M., Davies, T., 1993. Staging of gastrulating mouse embryos by morphological landmarks in the dissecting microscope. *Development* 118, 1255–1266.
- Dufort, D., Schwartz, L., Harpal, K., Rossant, J., 1998. The transcription factor *HNF3 β* is required in visceral endoderm for normal primitive streak morphogenesis. *Development* 125, 3015–3025.
- Eyal-Giladi, H., Kochav, S., 1976. From cleavage to primitive streak formation: a complementary normal table and a new look at the first stages of the development of the chick. *Dev. Biol.* 49, 321–337.
- Eyal-Giladi, H., 1997. Establishment of the axis in chordates: facts and speculations. *Development* 124, 2285–2296.
- Faust, C., Lawson, K.A., Schork, N.J., Thiel, B., Magnuson, T., 1998. The *Polycomb*-group gene *eed* is required for normal morphogenetic movements during gastrulation in the mouse embryo. *Development* 125, 4495–4506.
- Foley, A.C., Skromne, I., Stern, C., 2000. Reconciling different models of forebrain induction and patterning: a dual role for the hypoblast. *Development* 127, 3839–3854.
- Gallicano, G.I., Kouklis, P., Bauer, C., Yin, M., Vasioukhin, V., Degenstein, L., Fuchs, E., 1998. Desmoplakin is required early in development for assembly of desmosomes and cytoskeletal linkage. *J. Cell. Biol.* 143, 2009–2022.
- Gardner, R.L., 1997. The early blastocyst is bilaterally symmetrical and its axis of symmetry is aligned with the animal–vegetal axis of the zygote in the mouse. *Development* 124, 289–301.
- Harland, R., 2000. Neural induction. *Curr. Opin. Genet. Dev.* 10, 357–362.
- Ho, C.-Y., Houart, C., Wilson, S.W., Stainier, D.Y.R., 1999. A role for the extraembryonic yolk syncytial layer in patterning the zebrafish embryo suggested by properties of the *hex* gene. *Curr. Biol.* 9, 1131–1134.
- Jones, C.M., Broadbent, J., Thomas, P.Q., Smith, J.C., Beddington, R.S.P., 1999. An anterior signalling centre in *Xenopus* revealed by the homeobox gene *XHex*. *Curr. Biol.* 9, 946–954.
- Kimura, C., Yoshinaga, K., Tian, E., Suzuki, M., Aizawa, S., Matsuo, I., 2000. Visceral endoderm mediates forebrain development by suppressing posteriorizing signals. *Dev. Biol.* 225, 304–321.
- Knoetgen, H., Viebahn, C., Kessel, M., 1999. Head induction in the chick by primitive endoderm of mammalian, but not avian origin. *Development* 126, 815–825.
- Lawson, K.A., Pedersen, R.A., 1987. Cell fate, morphogenetic movement and population kinetics of embryonic endoderm at the time of germ layer formation in the mouse. *Development* 101, 627–652.
- Lawson, K.A., Meneses, J.J., Pedersen, R.A., 1991. Clonal analysis of epiblast fate during germ layer formation in the mouse embryo. *Development* 113, 891–911.
- Lu, C.C., Brennan, J., Robertson, E.J., 2001. From fertilization to gastrulation: axis formation in the mouse embryo. *Curr. Opin. Genet. Dev.* 11, 384–392.
- Piotrowska, K., Zernicka-Goetz, M., 2001. Role for sperm in spatial patterning of the early mouse embryo. *Nature* 409, 517–521.
- Rhin, M., Dierich, A., Shawlot, W., Behringer, R.R., Le-Meur, M., Ang, S.-L., 1998. Sequential roles for *Otx2* in visceral endoderm and neurectoderm for forebrain and midbrain induction and specification. *Development* 125, 845–856.
- Rodriguez, T.A., Casey, E.S., Harland, R.M., Smith, J.C., Beddington, R.S.P., 2001. Distinct enhancer elements control *Hex* expression during gastrulation and early organogenesis. *Dev. Biol.* 234, 304–316.
- Rosenquist, T.A., Martin, G., 1995. Visceral endoderm-1 (VE-1): an antigen marker that distinguishes anterior from posterior embryonic visceral endoderm in the early post-implantation mouse embryo. *Mech. Dev.* 49, 117–121.
- Shawlot, W., Wakamiya, M., Kwan, K.M., Kania, A., Jessell, T.M., Behringer, R.R., 1999. *Lim1* is required in both primitive streak-derived tissues and visceral endoderm for head formation in the mouse. *Development* 126, 4925–4932.
- Stern, C.D., Ireland 1981. An integrated experimental study of endoderm formation in avian embryos. *Anat. Embryol.* 163, 245–263.
- Tam, P.P.L., Steiner, K.A., 1999. Anterior patterning by synergistic activity of the early gastrula organizer and the anterior germ layer tissues in the mouse embryo. *Development* 126, 5171–5179.
- Thomas, P., Beddington, R., 1996. Anterior primitive endoderm may be responsible for patterning the anterior neural plate in the mouse embryo. *Curr. Biol.* 6, 1487–1496.
- Thomas, P.Q., Brown, A., Beddington, R.S.P., 1998. *Hex* a homeobox gene revealing peri-implantation asymmetry in the mouse embryo and an early transient marker of endothelial cell precursors. *Development* 125, 85–94.
- Varlet, I., Collingnon, J., Robertson, E.J., 1997. *Nodal* expression in the primitive endoderm is required for the specification of the anterior axis during mouse gastrulation. *Development* 124, 1033–1044.
- Viebahn, C., 1999. The anterior margin of the mammalian gastrula: comparative and phylogenetic aspects of its role in axis formation and head induction. *Curr. Top. Dev. Biol.* 46, 63–103.
- Viebahn, C., Mayer, B., Habre de Angelis, M., 1995. Signs of the principle body axes prior to primitive streak formation in the rabbit embryo. *Anat. Embryol.* 192, 159–169.
- Wilson, S.I., Edlund, T., 2001. Neural induction: toward a unifying mechanism. *Nat. Neurosci.* 4, 1161–1168.
- Zernicka-Goetz, M., 2002. Patterning of the embryo: the first spatial decisions in the life of a mouse. *Development* 129, 815–829.